Available online at www.sciencedirect.com
ScienceDirect
Chemical Physics Letters 445 (2007) 147–151
CHEMICAL PHYSICS LETTERS
www.elsevier.com/locate/cplett

Experimental and theoretical characterization of the $C^-_{n=2,16}$ clusters produced by 337 nm UV laser

Francisco Alberto Fernandéz-Lima [a,b,c], Cássia Ribeiro Ponciano [b], Enio Frota da Silveira [b], Marco Antonio Chaer Nascimento [a,*]

[a] Instituto de Química, Universidade Federal do Rio de Janeiro, Cidade Universitária, CT Bloco A, Sala 412, Rio de Janeiro, RJ 21949-900, Brazil
[b] Departamento de Física, Pontifícia Universidade Católica do Rio de Janeiro, Rua Marquês de São Vicente 225, C.P. 38071, Rio de Janeiro 22543-970, Brazil
[c] Instituto Superior de Tecnologias y Ciências Aplicada, Ave. Salvador Allende esq. Luaces, s/n, AP 6163, CP 10600, Ciudad de la Habana, Cuba

Received 30 June 2007; in final form 3 August 2007
Available online 11 August 2007

Abstract

The structures and abundances of $C^-_{n=2-16}$ clusters produced from amorphous and graphite targets by 337 nm UV laser are analyzed. A systematic search for the more stable conformers at the DFT/B3LYP level of calculation is presented. Two new series and some new structures of previously reported series of negatively charged carbon clusters are proposed: linear (new members), monocyclic (new members), fused ring and non-planar series. The cluster stability analysis indicates higher abundances for the $n = 2$, 4, 6, 8 and 12 clusters in the negative spectra, in agreement with the experimental observations.

1. Introduction

The study of pure carbon molecules has attracted great interest for many decades. Carbon clusters were first identified spectroscopically in the emission from interstellar clouds and other cosmic environments [1,2]. As shown in several reviews [3–6], the chemistry of C_n species has been the subject of intensive theoretical and experimental research [2,7–10]. In particular, a detailed knowledge of the physical and chemical properties of the carbon clusters is important for understanding a large variety of chemical systems such as: hydrocarbon flames, soot-forming, thin diamond and silicon carbide films and nanotubes production.

A number of methods (e.g., laser vaporization, electron impact, ion bombardment and sparks) and target materials (e.g., graphite, synthetic diamond, glassy carbon, carbon nanotubes, diamond-like films, condensed gases and organic polymers) have been used to produce neutral and single charged carbon clusters [11–18]. In experimental studies, carbon vaporization (with or without pos-ionization) yielded mass spectra with more abundant odd-numbered C^+_n and even-numbered C^-_n clusters [4,5,19–24] for n up to 10 as predicted by theory. Linear carbon chains are the most stable for ions with fewer than 10 atoms [25]. However, an interesting structural change seems to occur for clusters with $10 < n < 31$ as they appear to form cyclic structures [25]. Although stable C^+_n and C^-_n structures were first predicted to be non-cyclic, recent ab initio calculations ($n < 10$) predict stability also for some cyclic isomers [26].

In a previous work [27], we reported a systematic search for the most stable C^+_n conformers for $n = 2$–16. The isomers stabilities were compared with the experimental mass abundances for different carbon vaporization techniques. In [27], besides the linear and monocyclic series, new members of these series and two new series were described. The contribution of the stable isomers to the mass spectra for $n > 10$ was also discussed.

* Corresponding author. Fax: +55 21 2562 7265.
E-mail address: chaer@iq.ufrj.br (M.A.C. Nascimento).

0009-2614/$ - see front matter © 2007 Elsevier B.V. All rights reserved.
doi:10.1016/j.cplett.2007.08.023

In the present work, the distributions of carbon clusters produced by 337 nm UV laser on two different carbon targets (amorphous and graphite) are analyzed. Besides the target influence on the mass abundance, for a proper analysis of the conformers' stability, the neutral and negative spectra are simultaneously recorded. A systematic search for the stable C_n^- conformers, for $n = 2$–16, at the DFT/B3LYP/6-311G**++ level of calculation is presented and their contribution to the mass spectra intensities is discussed.

2. Experimental methods

The UV laser vaporization/ionization analysis was performed in the reflective and linear modes of a BRUKER/BIFLEX III mass spectrometer, equipped with a 337 nm UV nitrogen laser (3 ns FWHM, 200 μJ mean energy per pulse) from Laser Science Inc. A photodiode detects the laser pulse and generates the start signal for the TOF measurement. The C_n-desorption yields of the laser vaporization/ionization of the amorphous carbon (made by electron-sputtering deposition from a graphite carbon rod purchased from Le Carbone-Lorraine, France) and of graphite targets are presented in Fig. 1. Emitted negative ions were analyzed in the reflective mode (C_n^- ions) while those neutralized/dissociated ($(C_n)^*$ ions) on the flight were acquired simultaneously in the linear mode.

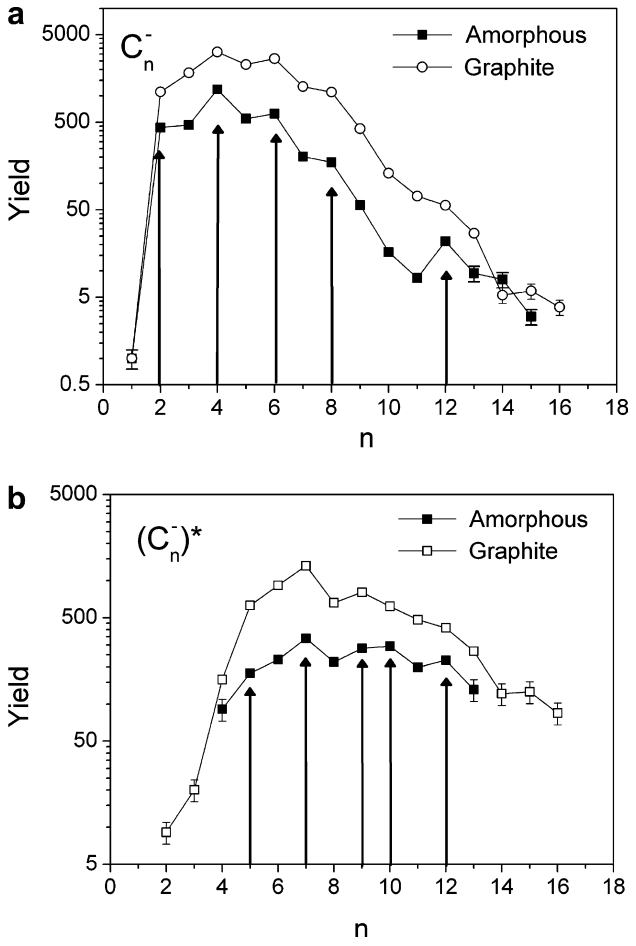

Fig. 1. Desorption yields (in semi-logarithmic plot) for the (a) negative C_n^- and (b) neutralized $(C_n^-)^*$ ion clusters produced by laser vaporization/ionization of an amorphous and graphite carbon target. Arrows indicate the higher abundances. The $(C_n^-)^*$ are the C_n^- emitted and accelerated ions that became neutral or dissociated in the linear TOF region.

3. Computational details

Negatively charged carbon clusters were calculated using DFT at the B3LYP/6-311G**++ level with the JAGUAR 6.0 software [28]. The basis set superposition error (BSSE) was found to be of the order of 0.02 eV. The accuracy of the B3LYP functional is known to be of the order of ~3 kcal/mol, meaning that conformers differing by less than that amount cannot be distinguished at this level of calculation. No symmetry restrictions have been imposed in the process of geometry optimization. A vibration analysis was performed in order to verify that the optimized structures correspond to real minima in the potential energy surfaces. The structures with $n < 6$ were also treated at the MP2/6-311G**++ level, since DFT calculations of negative ions are more susceptible to errors [29] due to the fact that, for the presently available functionals, the exchange energy does not exactly cancel the Coulombic self-interaction, this effect being more pronounced for the smaller structures. The MP2 results confirmed the geometries obtained at the DFT level.

4. Results and discussion

4.1. Series characteristics

Series I: All members of this series are linear clusters. As a general rule, the linear clusters are symmetric relative to the central atom, the inter-atomic distances varying from 1.269 to 1.308 Å.

Series II: The members of this series exhibit cyclic structures (Fig. 2 top). Except for $n = 5$, all members up to $n = 16$ were characterized at the level of calculation employed. For $n = 8$, 12 and 16, regular cyclic structures were obtained. The C_8^-IIa is a regular octagon with sides equal to 1.330 Å. The C_8^-IIb is a parallelogram with sides of (1.424 + 1.341) Å and an angle of 62.51° , with one carbon atom per vertex and one at the midpoint of each side of the parallelogram. The C_{12}^-II is a regular hexagon with sides of (1.326 + 1.274) Å and with one carbon atom at each vertex and one at the midpoint of each side of the hexagon. The C_{16}^-II is a regular octagon with sizes of (1.321 + 1.260) Å and a carbon atom per side and per vertex.

The inter-atomic distances of the linear and monocyclic clusters agree with the previously reported values, up to the second decimal place, for $n = 2$–4 [26] and $n = 7$ [29]. For $n = 4$ and 6 the linear structures are more stable than the monocyclic, in good agreement with the previously reported results [30,31].

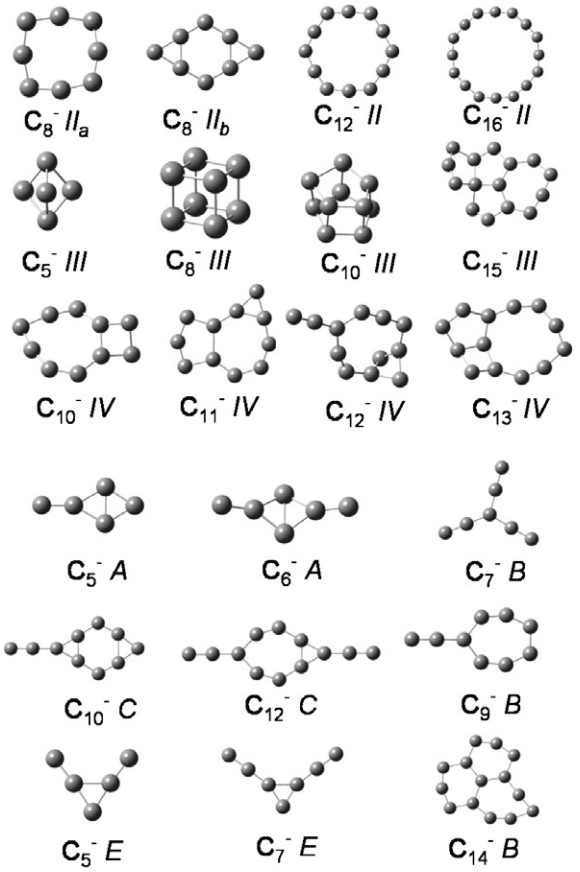

Fig. 2. Optimized geometries of some clusters at the DFT/B3LYP/6-311G**++ level of calculation.

Series III: The members of this series present non-planar structures (Fig. 2 top). The C_5^-III structure is a regular hexahedra with sizes of 1.507 Å. The C_8^-III is a perfect cube with sides of 1.505 Å. The C_{10}^-III structure is not strictly regular and is formed by two almost parallel pentagons. The C_{15}^-III structure is formed by three 5-membered and one 7-membered fused irregular carbon rings.

Series IV: The members of this series present fused ring structures. All the clusters are irregular rings with 4, 5, 8 and 9 members. The structures are all planar, except that of the C_{13}^- IV cluster.

Clusters A–C and E: The clusters labelled A (C_5^-A and C_6^-A) are characterized by the presence of a C_4 diamond-like structure to which carbon atoms are attached to along the axis containing the larger diagonal (Fig. 2 bottom). The negative charge is mainly located in the attached atoms. The clusters C_9^-B and C_{14}^-B are characterized for having a 7-membered ring. The C_7^-B structure has a central carbon atom to which three carbon dimers are symmetrically attached. Structures labelled C (C_{10}^-C and C_{12}^-C), are characterized by a C_8II core structure to which carbon dimers are attached along the axis containing the larger diagonal, analogously to the A clusters. The E labelled structures (C_5^-E and C_7^-E) are characterized by a C_3 core structure to which carbon atoms and dimers are attached, respectively.

Table 1
Carbon cluster internal energy $E_n(i)$, including ZPE correction, at the DFT/B3LYP/6-311G**++ level of calculation

Cluster	$E_n(i)$ (eV)	Cluster	$E_n(i)$ (eV)	Cluster	$E_n(i)$ (eV)
C^0	−1028.37	C_7^-B	−7251.07	C_{11}^-IV	−11 393.61
C_1^-	−1029.98	C_7^-E	−7249.83	C_{12}^-I	−12 434.82
C_2^-I	−2069.62	C_8^-I	−8289.15	C_{12}^-II	−12 434.00
C_3^-I	−3106.12	C_8^-IIa	−8286.41	C_{12}^-IV	−12 430.05
C_3^-II	−3105.56	C_8^-IIb	−8286.35	C_{12}^-C	−12 431.00
C_4^-I	−4143.10	C_8^-III	−8281.91	C_{13}^-I	−13 471.11
C_4^-II	−4141.34	C_9^-I	−9325.46	C_{13}^-II	−13 471.40
C_5^-I	−5179.50	C_9^-II	−9324.02	C_{13}^-IV	−13 466.64
C_5^-III	−5175.32	C_9^-B	−9323.18	C_{14}^-I	−14 507.59
C_5^-A	−5177.06	C_{10}^-I	−10 362.00	C_{14}^-II	−14 508.32
C_5^-E	−5176.34	C_{10}^-II	−10 361.51	C_{14}^-B	−14 504.34
C_6^-I	−6216.21	C_{10}^-III	−10 354.20	C_{15}^-I	−15 543.87
C_6^-II	−6214.48	C_{10}^-IV	−10 357.39	C_{15}^-II	−15 543.11
C_6^-A	−6211.56	C_{10}^-C	−10 358.85	C_{15}^-III	−15 535.94
C_7^-I	−7252.53	C_{11}^-I	−11 398.30	C_{16}^-I	−16 580.35
C_7^-II	−7250.17	C_{11}^-II	−11 397.52	C_{16}^-II	−16 580.68

The energies for all the stable conformers are shown in Table 1.

4.2. Cluster abundance

The analysis of the experimental data presented in Section 2 is aimed at elucidating the dependence of the cluster production/ionization and stability on the target structure, for 337 nm UV laser pulses as the vaporization source. For both amorphous and graphite targets, the experimental yields of the negatively charged carbon clusters (C_n^-) present a Maxwell–Boltzmann type distribution [27] centred at $n = 5$. For the neutral carbon clusters (C_n) produced by fragmentation or neutralization of the emitted C_n^- clusters, the experimental yields also show a Maxwell–Boltzmann type distribution, for both targets, but centred at $n = 7$.

The experimental yields of clusters originated from the amorphous target are one order of magnitude lower than those from the graphite target. However, for both targets the mass spectra show relative higher abundances at $n = 2$, 4, 6, 8 and 12 in the negatively charged carbon spectra. In the neutral spectra, relative higher abundances are observed for $n = 5$, 7, 9, 10, 12 and 15. The relative higher abundances for the ionized species correlate with the relative lower abundance in the neutral spectra.

4.3. Cluster stability

The abundance of the emitted clusters (or the yield, Y) is a function of the production mechanism (P), the ionization mechanism (I) and the stability (S) of the clusters: $Y = F(P, I, S)$ [32]. The introduction of the stability function S_n can be helpful in analyzing the cluster abundance variation.

The stability function is defined as the second variation of the cluster total energy E_n including the zero-point energy correction: $S_n \equiv E_{n-1} + E_{n+1} - 2E_n$. Assuming that all clusters have the same probability of being produced

and ionized, it is reasonable to expect that the more stable ones should be also the more abundant ones.

The results of the analysis performed by applying the stability function separately to the members of series I and II, and also considering a set of structures formed by the lower energy isomers of series I and II are presented in Fig. 3 top. The stability analysis using only the members of series I shows an even/odd periodicity for $n = 2$–15, the even structures being the most stable ones. This result agrees with the previously reported data [25,26]. In the case of series II, the analysis was performed for n larger than 5, since the cyclic pentamer is not stable. The stability analysis for the members of this series shows a higher abundance for $n = 10$ and 14. Considering only the lower energy isomers among the structures of series I and II, the stability analysis also predicts the even-numbered clusters as the most stable ones (Fig. 3 top). Except for $n = 10$, the stability analysis using the lower energy structures of series I and II agrees with the experimental mass abundance (negative spectra). Two possible explanations for the disagreement found for $n = 10$ are: (i) in spite of the systematic search performed, other lower energy structures are possible for $n = 9$ and 11; and (ii) either the production or the ionization process is more effective for $n = 10$. The latter, and more likely, explanation can be probed by a simple analysis of the cluster occurrence, as discussed below.

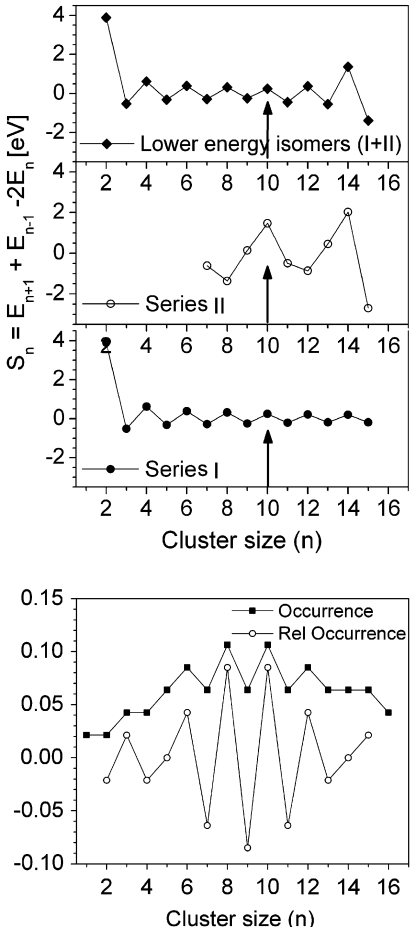

Fig. 3. (top) Stability analysis for series I and II and the low energy isomers of series (I + II); (bottom) the cluster occurrence (O_n) and relative occurrence ($2O_n - O_{n-1} - O_{n+1}$) as a function of the cluster size.

4.4. Cluster occurrence

Let us define the occurrence of a cluster of size n (O_n), as the number of possible stable isomers for a given value of n divided by the total number of stable structures predicted by the calculations. If one considers that all the clusters have the same probability of being produced and ionized, the most abundant ones should correspond to values of n for which a larger number of stable isomers is possible. This assumption is partially supported by the independence of the cluster relative abundances on the target structure, as previously shown (Fig. 1). The fact that the relative abundances are independent of the target structure can be related to the condensation mechanism of cluster formation [27,33–35] since the condensation probability for a cluster of size n also grows with the number of possible n-isomers.

The species observed in the neutral spectrum are those from the fragmentation and/or neutralization of the meta-stable ions desorbed from the target. The occurrence as a function of the cluster size is larger for $n = 5$–15 (Fig. 3 bottom) and agrees well with the cluster abundance in the neutral spectra. The odd–even abundance correspondence between the negative and neutral spectra and those predicted by the stability analysis (considering the lower energy isomers of series I and II) is observed except for the $n = 10$ and $n = 12$ clusters.

One might expect the abundance for the $n = 12$ clusters in the neutral spectra to be higher than that for the $n = 10$ ones since the probability of neutralization increases with the size of the cluster. However, since the occurrence for $n = 10$ is larger than for $n = 12$, the overall probability of neutralization could be higher for $n = 10$. Therefore, it is possible that the $n = 10$ lower abundance in the negative spectra and the $n = 10$ and $n = 12$ large abundances in the neutral spectra are due to the neutralization of these clusters in the time-of-flight region.

5. Conclusions

Four series of carbon clusters for $n = 2$–16 are identified in the systematic search performed at the DFT/B3LYP/6-311G**++ level. Besides the new members of the linear and monocyclic series ($n > 10$), two new series (fused ring and non-planar series) and some new isomers (labelled A–E) are presented. The analyzed carbon structures, amorphous and graphite, show no influence on the relative mass abundance on the negative and neutral species spectra. Except for $n = 10$, the experimental mass abundances are well described by the stability function analysis using the low energy isomers ($n = 2$, 4, 6, 8 and 12). The disagreement observed for $n = 10$ is possibly due to a higher probability of neutralization of these clusters in the time-of-

flight region, since a larger number (occurrence) of stable $n = 10$ isomers can be formed.

Acknowledgements

The authors acknowledge the financial support by CNPq, FAPERJ, PRONEX, CLAF and Instituto do Milênio de Materiais Complexos.

References

[1] P.F. Bernath, Science 244 (1989) 562.
[2] H.W. Kroto, Science 242 (1988) 1139.
[3] W.A. Chupka, M.G. Inghram, J. Chem. Phys. 22 (1954) 1472.
[4] D.M. Cox, K.C. Reichmann, A. Kaldor, J. Chem. Phys. 88 (1988) 1588.
[5] W. Weltner Jr., R.J. Vanzee, Chem. Rev. 89 (1989) 1713.
[6] A.V. Orden, R.J. Saykally, Chem. Rev. 98 (1998) 2313.
[7] R.F. Curl, R.E. Smalley, Science 242 (1988) 1017.
[8] J.L. Robertson, S.C. Moss, Y. Lifshitz, S.R. Kasi, J.W. Rabalais, G.D. Lempert, E. Rapaport, Science 243 (1989) 1047.
[9] W.A. Yarbrough, R. Messier, Science 247 (1990) 688.
[10] H.W. Kroto, J. Chem. Soc., Faraday Trans. 86 (1990) 2465.
[11] E.A. Rohlfing, D.M. Cox, A. Kaldor, J. Chem. Phys. 81 (1984) 3322.
[12] W.R. Creasy, J.T. Brenna, J. Chem. Phys. 92 (1990) 2269.
[13] Y. Zhang, S. Iijima, Appl. Phys. Lett. 75 (1999) 3087.
[14] O. Sedo, M. Alberti, J. Janca, J. Havel, Carbon 44 (2006) 840.
[15] J.J. Gaumet, A. Wakisaka, Y. Shimizu, Y. Tamori, J. Chem. Soc., Faraday Trans. 89 (1993) 1667.
[16] H. Feld, R. Zurmuhlen, A. Leute, A. Benninghoven, J. Phys. Chem. 94 (1990) 4595.
[17] G. Brinkmalm, P. Demirev, D. Fenyo, P. Hakanson, J. Kopniczky, B.U.R. Sundqvist, Phys. Rev. B 47 (12) (1993) 7560.
[18] C.R. Ponciano et al., J. Am. Soc. Mass Spectrom. 17 (2006) 1120.
[19] M.G. Giuffreda, M.S. Deleuze, J.-P. Francois, J. Phys. Chem. 103 (1999) 5137.
[20] M.J. Deluca, M.A. Johnson, Chem. Phys. Lett. 152 (1988) 67.
[21] A.N. Pargellis, J. Chem. Phys. 93 (1990) 2099.
[22] P.P. Radi, M.E. Rincon, M.T. Hsu, J. Brodbelt-Lustig, P.R. Kemper, M.T. Bowers, J. Phys. Chem. 93 (1989) 6187.
[23] C. Lifshitz, P. Sandler, H.F. Grutzmacher, J. Sun, T. Weiske, H. Schwarz, J. Phys. Chem. 97 (1993) 6592.
[24] S.B.H. Bach, J.R. Eyler, J. Chem. Phys. 92 (1990) 358.
[25] S. Yang, K.J. Taylor, M.J. Crayraft, J. Conceição, C.L. Pettictte, O. Cheshnovsky, R.E. Smalley, Chem. Phys. Lett. 144 (1988) 431.
[26] A. Fura, F. Turecek, F.W. McLafferty, Int. J. Mass Spectrom. 217 (2002) 81.
[27] F.A. Fernandez-Lima, C.R. Ponciano, E.F. da Silveira, M.A.C. Nascimento, Chem. Phys. Lett. 426 (2006) 351.
[28] Jaguar 5.5 and 6.0, Schroedinger Inc., Protland, OR, 2004.
[29] N. Rosch, S.B. Trickey, J. Chem. Phys. 106 (1997) 8940.
[30] S. Schmatz, P. Botschwina, Int. J. Mass Spectrom. Ion Process. 99 (1995) 10736.
[31] J.D. Watts, I. Cernusak, R.J. Barlett, Chem. Phys. Lett. 178 (1991) 229.
[32] R.L. Johnston, Atomic and Molecular Clusters, Taylor & Francis, London, 2002.
[33] F.A. Fernandez Lima, C.R. Ponciano, H.D. Fonseca Filho, E. Pedrero, M.A. Chaer Nascimento, E.F. da Silveira, Appl. Surf. Sci. 252 (2006) 8171.
[34] V.M. Collado, F.A. Fernandez-Lima, C.R. Ponciano, M.A.C. Nascimento, L. Velazquez, E.F. da Silveira, Phys. Chem. Chem. Phys. 7 (2005) 1971.
[35] F.A. Fernandez Lima, V.M. Collado, C.R. Ponciano, L.S. Farenzena, E. Pedrero, E.F. da Silveira, Appl. Surf. Sci. 217 (2003) 202.